Journal of Radioanalytical and Nuclear Chemistry
https://doi.org/10.1007/s10967-020-07270-x

Inorganic silica gel functionalized tris(2-aminoethyl)amine moiety for capturing aqueous uranium (VI) ion

Mohammed A. Al-Anber[1] · Idrees F. Al-Momani[2] · Mohammed A. Zaitoun[3] · Wala' Al-Qaisi[1]

Received: 13 April 2020

Abstract
The silica gel functionalized tris(2-aminoethyl)amine moiety (SG-TAEA-NH_2) has been successfully used for capturing aqueous uranium ion by batch sorption. Various sorption experiments are performed using several variables such as pH, initial concentration, contact time, and temperature. These variables enable us to study the thermodynamic and kinetic of sorption, which in turn, leads to know more about the interaction and behavior of the uranium ion on the surface. The equilibrium of sorption can be achieved within the first $t = 5$–10 min upon the study conditions ($C_i = 1$ mg L^{-1}, $T = 25$ °C, 80 rpm, $pH_i = 7$, and dosage = 2 g L^{-1}). The sorption of U(IV) ion onto the surface of SG-TAEA-NH_2 material. The sorption of U(VI) ion follows the Freundlich isotherm model ($R^2 > 0.999$). The motivation of sorption is due to the chemisorption of U(IV) ion onto an amino-active site forming a complex in the surface, which is proven through the values of (1) the Dubinin–Kaganer–Radushkevich sorption energy (ca. $E = -24$ to -36), (2) the pseudo-second-order kinetic model ($R^2 > 0.999$) and (3) the spectrum of the FTIR. The rate constant and sorption capacities are calculated. Based on these promising results, we recommend using SG-TAEA-NH_2 as an effective adsorbent and filter to remove uranium ion from the water up to 99%.

Keywords Silica gel · Tris(2-aminoethyl)amine · Uranium ion · Sorption · Freundlich isotherm · Pseudo-second order

Introduction

Jordanian governments tend to build nuclear reactors for peaceful purposes such as research purposes and to generate electricity. Uranium is considered the main source for the operation of nuclear plants, as a nuclear fuel in nuclear water, to generate energy. However, it is possible to produce amounts of the nuclear power reactor effluents containing uranium ion [1, 2]. When conditions are available and sufficient to oxidize uranium element turns into enriched uranyl ion (UO_2^{2+}) [3–5]. Generally, uranium exists in solution as soluble UO_2^{2+} ion in the form of carbonate complexes $(UO_2)_2CO_3(OH)_3^-$, $UO_2CO_3^\circ$, $UO_2(CO_3)_2^{2-}$, $UO_2(CO_3)_3^{4-}$ and possibly $(UO_2)_3(CO_3)_6^{6-}$ [6] and hydrolysis ion such as $[UO_2(OH_2)_5]^{2+}$ [5, 7, 8]. However, uranium and uranium ion can cause a threat for both the human body and environment because it has chemical toxicity and radioactivity. The presence of a high concentration of UO_2^{2+} ion in drinking water can accumulate in some human body organs such as kidney, liver, lung, and bone, causing serious risks like cancer disease and renal frailer (kidney damage) [9–14]. The EPA has set the level of safe contamination of uranium ion to be lower than 30 µg L^{-1}. Thus, the concentration of uranium ion in water (e.g. UO_2^{2+} ion) must be reduced to the recommended limit as well as selectively capturing within a safe framework structure. This research work can help us to remove the toxic uranium ions from nuclear water effluents as well as to re-concentrates it for another use.

Various techniques are used to remove UO_2^{2+} ion from water, including solvent extraction [15, 16], coagulation-filtration [17], lime softening [18], electrolytic reduction [19], ion exchange [20–22], chemical precipitation [23], reverse osmosis [24], altra-filtration [25], membrane and electrodyalysis [26, 27], chromatographic extraction [28], flotation [29] and adsorption. Different adsorbents are widely utilized for uranium (VI) ion from water [30]. The importance of utilizing different type of adsorbents is due to the efficiently,

✉ Mohammed A. Al-Anber
masachem@mutah.edu.jo

[1] Department of Chemistry, Faculty of Sciences, Mutah University, P.O. Box 7, Al-Karak 61710, Jordan

[2] Department of Chemistry, Faculty of Sciences, Yarmouk University, Irbid, Jordan

[3] Department of Pharmaceutical Sciences, Faculty of Pharmacy, Yarmouk University, Irbid, Jordan

Published online: 09 July 2020

flexibility, safely, economical visibility, simplicity and lower environmental health impact. There are pieces of examples such as mesoporous silica [31], nanoporous silica [32], synthetic resin [33], covalent organic framework [34], chitosan and cross-linked chitosan [35, 36], polypyrole [37], composite adsorbents [38],silicon dioxide nanopowder [39], inorganic oxides nanosheets or nanofibers [40, 41], biomasses [42–44], hydroxyapatite [45, 46], activated carbon [47–49], carbon nanotubes [50], graphene oxide and its amine-functionalized composite [51], zero-valent iron [52, 53], polyamidoxime-functionalized colloidal particles [54], amino-functionalized urea–formaldehyde framework mesoporous silica [55], titania nanoparticles covalently functionalized with simple organic ligands [56], porous magnetic N-doped Fe/Fe_3C at carbon matrix and its highly efficient uranium(VI) remediation [57], and iron oxides [58–61], hematite [62] oxine functionalized magnetic Fe_3O_4 particles [63] and activated silica gel [64]. Uranium extraction by sulfonated mesoporous silica derived from blast furnace slag [65] montmorillonite, [66] hydroxide/graphene hybrid material [67] Manganese Oxide coated zeolite [68] amidoxime functionality within a mesoporous imprinted polymer material [69], Tendurek volcanic tuff [70].

These methods do not succeed in terms of selectivity and high cost, as well as are not easy to handle. From another direction, the natural adsorbents and their biomasses are economically effective and easy to handle. Nevertheless, in terms of selectivity, it is not. To achieve higher selectivity in capturing uranium ions from water, the silica gel functionalized organic or inorganic entities could be the best choice. Recently, the removal of uranium(VI) from water has been reviewed [71]. In terms of selectivity, the removal of uranium(VI) ion was investigated using amidoxime silica [72]. Other recent pieces of works on the market deal with utilizing silica gel functionalized organic or inorganic entities for capturing uranium ion from water. For example, silicate nanotubes [64, 73, 74], ethylene-di-amine-tri-acetate [75], amine-modified silica gel [76], murexide [77], silica gel or silica-gel-bound macrocycles [78, 79] and organic or inorganic polymeric ion exchangers [80–83].

Recently, Huang et al. have used tris(2-aminoethyl)amine ligand to modify the surface of silica gel. Wherein, it shows a high affinity for selective sorption Cr(III), Cd(II), and Pb(II) ions from water [84]. Besides, our group has found a highly efficient of such SG-TAEA-NH_2 material for capturing of a single ion phase of the ferric ion [85]. As the continuity of this recent work, we are still studying the efficiency of this adsorbent to capture a single phase of metal and heavy metal ions from water. It is important to indicate that we have not found any study related to the utilization of silica gel particles functionalized tris(2-aminoethyl) amine moiety (SG-TAEA-NH_2) for the sorption of aqueous UO_2^{2+} ion. Herein, we are still studying the efficiency of this adsorbent to capture a single phase of U(VI) ion from water. The novelty of this study lies in understanding the mechanism of adsorption and the bonding of uranium ion into the surface of SG-TAEA-NH_2. This can provide us a complete knowledge and view regarding the selectivity capturing uranium ion from water, which can help us to understand the sorption mechanism in case of the binary ions phase of the next study. In this contribution, we use SG-TAEA-NH_2 solid particles for capturing and sorption the aqueous UO_2^{2+} ion from water. The distribution of uranium(VI) ion between the aqueous phase and the SG-TAEA-NH_2 solid phase can be investigated. The adsorption data of the various experiments can be analyzed by adsorption kinetics and isotherm models.

Materials and methods

Preparation of silica gel functionalized tris(2-aminoethyl) amine moiety (SG-TAEA-NH_2)

The silica gel functionalized tris(2-aminoethyl)amine moiety (SG-TAEA-NH_2) was prepared according to the reported literature [84]. A summary of the preparation method has been recently published [85]. The surface proposed structure of the tris(2-aminoethyl) amine-functionalized silica gel (SG-TAEA-NH_2) is demonstrated in Scheme 1.

Reagents

The analytical grade uranyl acetate ($UO_2(CH_3COO)_2{\cdot}2H_2O$) was provided from Polysciences GmbH. Other reagents, the preparation of the stock solution (100 mg L^{-1}) of UO_2^{2+} ion, and the methodology of the experiments have been reported [85]. Arsenazo-III (3,6-bis[(2-arsonophenyl)azo]-4,5-dihydroxy-2,7-naphthalenedisulfonic acid) (Fluka Chemie, Buchs, Switzerland). Perchloric acid (70%) purchased from Sigma-Aldrich.

Apparatus and instruments

All absorbance measurements of the electronic spectra were made on A Shimadzu UV/Vis-1800 spectrophotometer (Shimadzu, Tokyo, Japan) with 1-cm quartz cells was used for measurement of the absorbance. The concentration of U was investigated by a spectrophotometric method using arsenazo(III) as a chromogenic reagent. Arsenazo III (Sigma-Aldrich): (0.07% w/v) solution was prepared in 3 M $HClO_4$.

Uranium standard solution (1000 mg L^{-1} U (w/v)): This solution can be prepared by dissolving uranyl nitrate hexahydrate (Riedel-de-Haen, Switzerland) in 3 M $HClO_4$. In a 10 ml standard volumetric flask, 2 ml of the sample containing U(VI) and 3 ml of the 0.07% (w/v) arsenazo III solutions were mixed. The contents of the flask were made

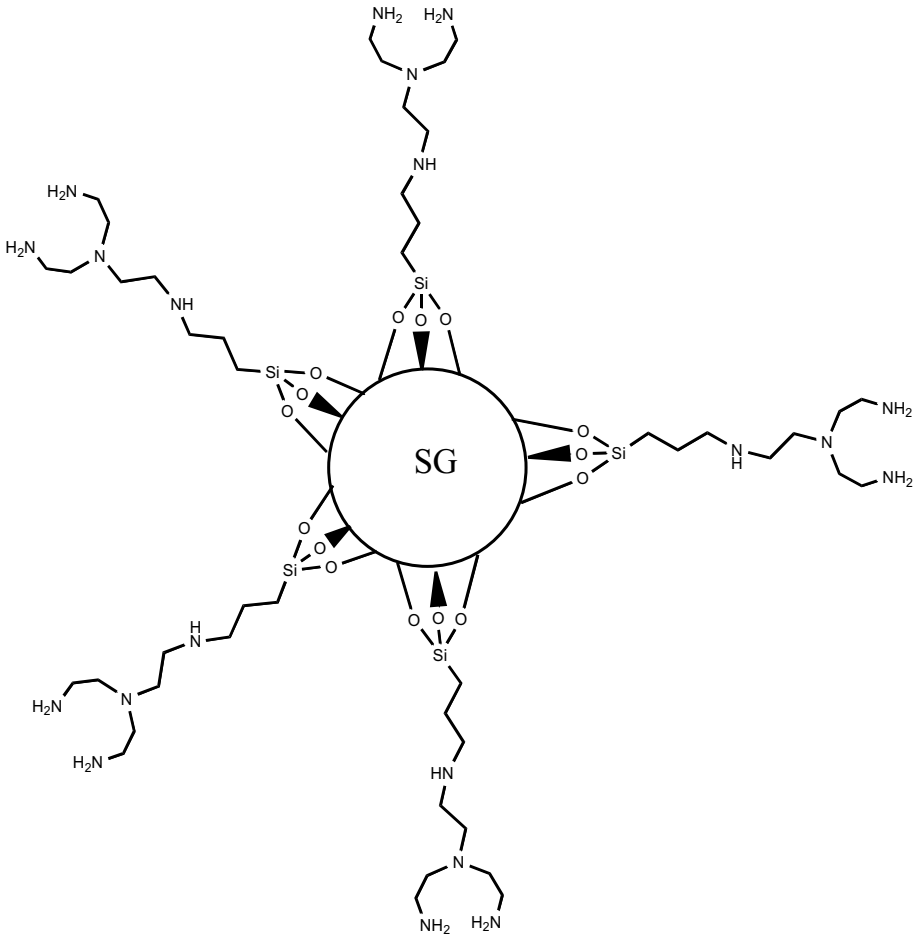

Scheme 1 The proposed structure of the tris(2-aminoethyl) amine-functionalized silica gel (SG-TAEA-NH_2) [85]

up to the mark with 6 M $HClO_4$ solution to ensure a final concentration of 3 M for $HClO_4$. After shaking the sample, the absorption can be measured against the reagent blank at 651 nm [86].

Equilibrium studies

The adsorbed amount of the UO_2^{2+} ion onto the SG-TAEA-NH_2 at equilibrium and in a specific t is q_e and q_t (mg g^{-1}), which are calculated by Eqs. 1 and 2, respectively.

$$q_e = \frac{(C_i - C_e)}{S} \tag{1}$$

$$q_t = \frac{(C_i - C_t)}{S} \tag{2}$$

where C_i, C_e, and C_t are the initial, the equilibrium, and the final concentration at a specific time of UO_2^{2+} ion in the aqueous solution (mg L^{-1}), respectively.

The dosage (S) of SG-TAEA-NH_2 can be calculated by Eq. 3:

$$S = \frac{m}{v} \tag{3}$$

where ν and m are the initial volume of UO_2^{2+} ion solution and the mass of SG-TAEA-NH_2 adsorbent, respectively.

The percentage removal of uranium ion can be calculated by Eq. 4:

$$\%\ \text{Removal of U(VI) ion} = \frac{C_i - C_e}{C_i} \times 100\%. \tag{4}$$

The distribution ratio (K_d) can be clarified in Eq. 5:

$$K_d = \frac{\text{Amount of U(VI) ion in SG - TAEA - NH}_2}{\text{Amount of U(VI)ion in solution}} \times \frac{1}{S}. \tag{5}$$

wherein, the relationship between the adsorption percentages and K_d (L g^{-1}) is presented in Eq. 6:

$$\%\ \text{of Adsorption} = \frac{1000K_d}{K_d + \frac{1}{S}}. \tag{6}$$

Batch sorption experiment

The sorption performance of SG-TAEA-NH_2 material toward the sorption of the uranium (VI) ion was tested by using the batch system at specific $T = 35$ °C (± 1 °C) with changing in C_i (1, 5, 10, and 20 mg L^{-1}) or at specific $C_i = 10$ with changing T (25, 35, 45, and 55 °C). The closed sorption system containing 2 g L^{-1} of SG-TAEA-NH_2 was shaken vigorously (*rpm* of the thermostatic mechanical shaker = 80) of up to 180 min. Afterward, the supernatant solution must be filtered by using filter paper (Whatman No. 41). The filtrate solutions can be analyzed by recording the average of at least triplicate measurements as mention in our reported experiment [85].

Result and discussion

FT-IR spectra

The silica gel functionalized tris(2-aminoethyl)amine moiety (SG-TAEA-NH_2) are mainly composed of silica gel and organic entities, which contain a variety of functional groups. The main functional groups in the FTIR spectrum are Si–O–Si and CH_2, primary and secondary NH_2, which have been recently discussed [85]. After heavy uranium (VI) ion sorption, some changes can be observed in the FTIR spectrum of SG-TAEA-NH_2 material. Therefore, the FTIR spectra can be also used as evidence of the chemisorption and complex formation in the surface by controlling the shift in the stretching frequency of the primary and secondary NH_2. In particular, Fig. 8 shows the bending vibration of primary amine ($\delta_{N-H}{}^{primary}$) at 1594.4 cm^{-1}, which is shifted by $\Delta\delta = 69$ cm^{-1} in contrast to the SG-TAEA-NH_2 ($\delta_{Nz-H}{}^{primary} = 1525$ cm^{-1}) before adsorption. The stretching ($\nu_{N-H}{}^{primary}$) is 3321 cm^{-1}, which is cannot be observed due to the weakness of peak transmittance. These changes and shifts in peak positions suggest the presence of the chemical interaction and a possible complexation reaction between the uranium(VI) ion and NH_2 moiety in the SG-TAEA-NH_2 surface [87]. These results are consistent with the mechanisms proposed for the removal of iron ion [85] (Fig. 1).

Effect of pH

Figure 2 shows that the sorption of uranium (VI) ion by the SG-TAEA-NH_2 matrix increase dramatically with increasing pH to the maximum 99% at pH = 7–8, as no further increase above this pH value. This result matches the reported one regarding the adsorption of uranium on the amidoxime resins [88], modified carbon nanotubes [89], and polyacrylhydroxamic acid sorbent [90].

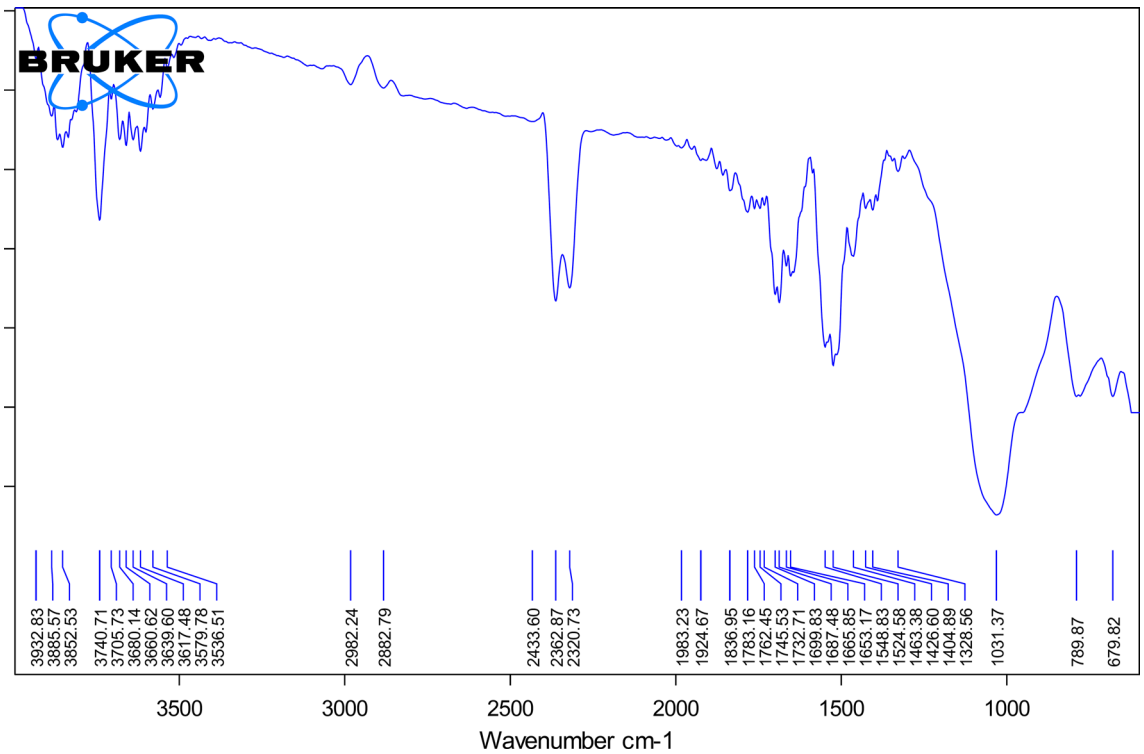

Fig. 1 ATR-IR spectrum for the SG-TAEA-NH2-U(VI) after 20 min of sorption $C_i = 10$ mg L^{-1} at 25 °C

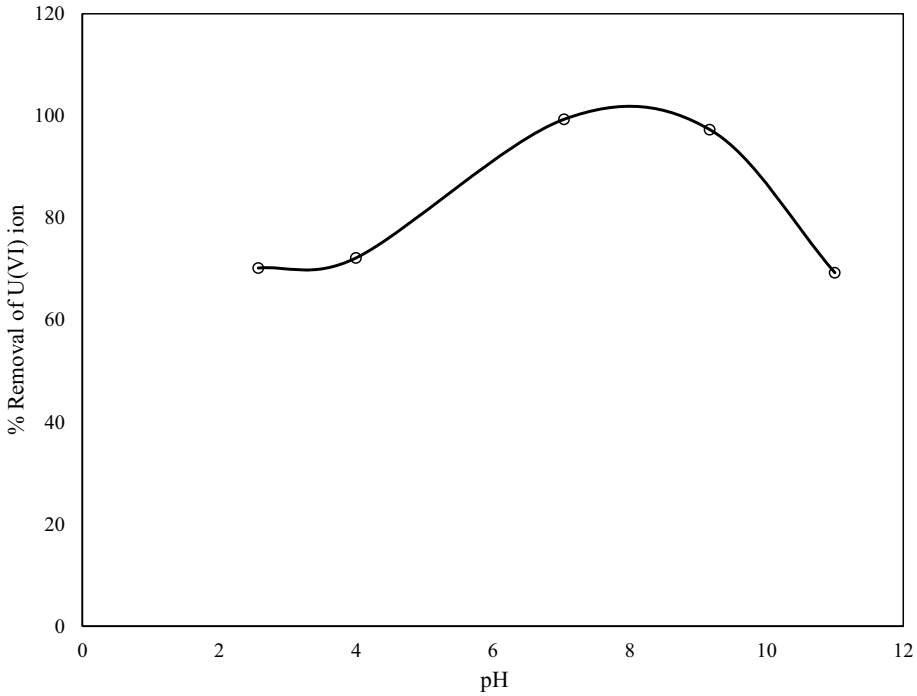

Fig. 2 The effect of pH on the capture of uranium (VI) ion from water by using Silica Gel functionalized tris(2-aminoethyl)amine moiety, $T = 25$ C, dosage = 2 g L^{-1}, 80 rpm, and $C_i = 10$ mg L^{-1}, $t = 5$ min

The pH has a significant role in the sorption and binding of U(VI) ion with amino-entity in the inorganic silica gel of the SG-TAEA-NH_2 surface. Furthermore, the pH effects in both the stability of the U(VI) ion (complex species) and the SG-TAEA-NH_2 surface morphology (protonation of the amino-entity). Therefore, to understand the effect of pH on the sorption behavior of U(VI) ion onto the SG-TAEA-NH_2 surface, we have studied the sorption using the basic, neutral, and acidic medium.

In an acidic medium (pH < 7), there is a high concentration of H^+ cation, which competes UO_2^{2+} ion (pH < 5) for binding in the amino-entity active sites. However, the functional amino-entity is protonated to be $–NH^{3+}$. This can block and shield the attraction of di-cationic UO_2^{2+} ion toward the positively charged surface. However, the competition of proton (H^+) cation for the amino-entity active sites decreases by increasing the pH (1 > pH > 7). Wherein, this can enhance the interaction and sorption of U(VI) ion onto the SG-TAEA-NH_2 surface forming SG-TAEA-NH_2… U complex.

In a basic medium (pH > 7), uranium (VI) ion gradually hydrolyzed to form a mono-cationic complex of $UO_2(OH)^+$. The mono-cationic complex has less affinity of interaction with amino-entity on the surface than the di-cationic uranyl ion (UO_2^{2+}: pH < 5). Therefore, the sorption affinity of $UO_2(OH)^+$ cation with the SG-TAEA-NH_2 matrix at basic is less than acidic and neutral medium. This agrees with the reported work regrading the sorption of uranium (VI) ion from nuclear industrial effluent by using nanoporous silica adsorbent [91]. At 7 ≤ pH ≤ 11, Uranium (VI) can be found in the form of $UO_2(OH)_2{\cdot}H_2O$ neutral molecule [92], and wood powder and wheat straw [93].

The acidic medium can affect directly the SG-TAEA-NH_2 matrix forming a shield of positive charges against the sorption of di-cationic UO_2^{2+} ion. From another direction, the basic medium can decrease this positive shield on the SG-TAEA-NH_2 matrix, but forming a mono-cationic $UO_2(OH)^+$The acidic medium can afect directly complex. These two opposite factors guiding us to conclude that the capturing of uranium (VI) is not favorable in both acidic and basic medium to achieve the maximum removal. Therefore, we have chosen pH = 7–8 as an optimum pH for capturing of uranium (VI) onto the SG-TAEA-NH_2 matrix.

Effect of initial concentration

The batch sorption technique is used for all experiments at 35 (± 1 °C). Different initial concentrations of UO_2^{2+} ion ($C_i = 1$, 5, 10, and 20 mg L^{-1}) are used of up to 3.0 h. All other sorption parameters are kept constant (e.g. $pH_i = 7$, $T = 25$ °C and 2 g L^{-1} dosage of SG-TAEA-NH_2 materials). Figure 3 shows the effect of initial concentration, wherein the percentage of capturing uranium (VI) ion from solution decreases with increasing the initial concentration of uranium (VI) ion in solution. For example, the maximum percentage of capturing uranium (VI) ion achieve 98% at $C_i = 1$ mg L^{-1}, while it is 93% at $C_i = 20$ mg L^{-1}. This is due to the availability the sufficient amino-active sites into the SG-TAEA-NH_2 matrix. For a given SG-TAEA-NH_2 particle dose, the total

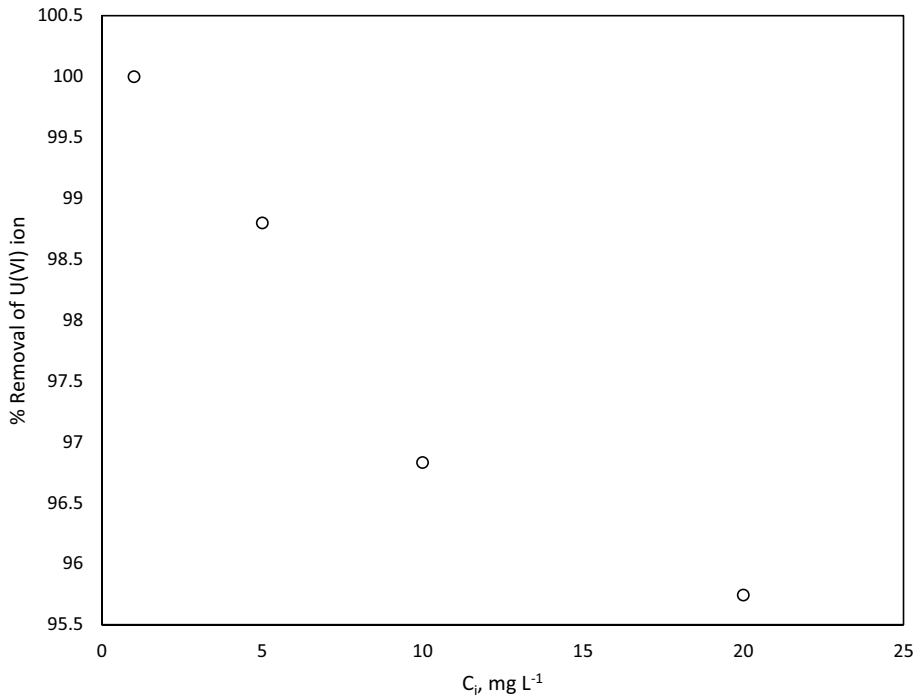

Fig. 3 The effect of initial concentration (C_i) on the capture of uranium (VI) ion from water by using Silica Gel functionalized tris(2-aminoethyl)amine moiety, $T = 25$ °C, dosage = 2 g L^{-1}, 80 rpm, and $C_i = 1$, 5, 10 and 20 mg L^{-1}, pH = 7, $t = 5$ min

number of amino-active sites available is fixed; wherein, the fixed amount adsorb almost the equal amount of uranium (VI) ion. This results in a decrease in the removal of uranium (VI) ion inconsequent to an increase in the initial uranium (VI) ion concentration. Furthermore, due to the increasing of competing of U(VI) cation onto the active sites of the SG-TAEA-NH_2 matrix. This agrees with what reported previously regarding the utilization of wood powder and wheat straw [93].

Effect of temperature

The effect of temperature is studied over a variant $T = 25$, 35, 45, and 55 °C. Wherein, 50 mL of 10 mg L^{-1} of UO_2^{2+} ion and 2 g L^{-1} of TAEA-SiO_2 solid materials were shaken vigorously and controlled through a period of up to 3 h and $pH_i = 7$. The percentage of capturing uranium (VI) ion increase with the increase of temperature as shown in Fig. 4. The maximum percentage of capturing uranium (VI) ion is 99% at $T = 55$ °C, while it is 93% at $T = 25$ °C. This is in line

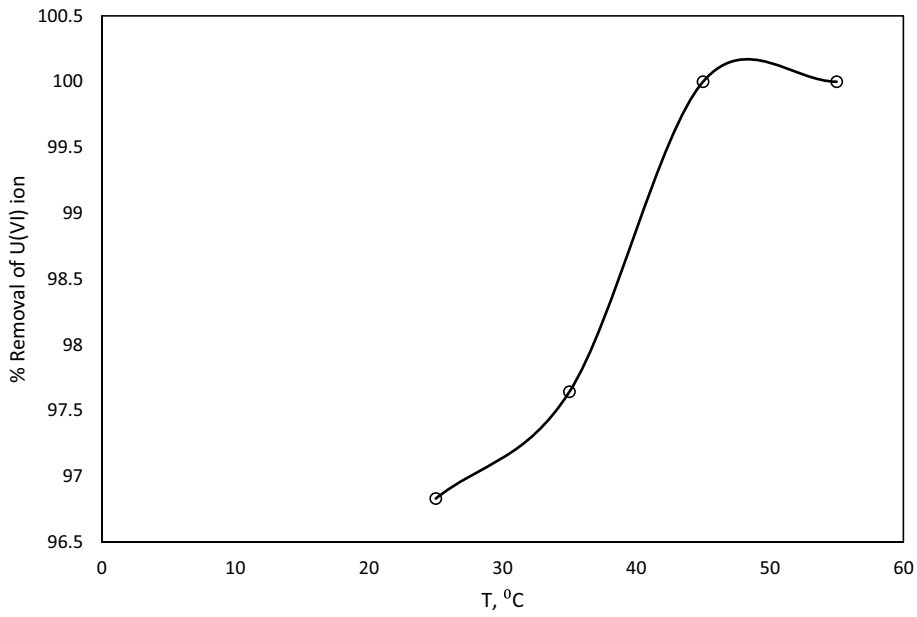

Fig. 4 The effect of Temperatures on the capture of uranium (VI) ion from water by using Silica Gel particles functionalized tris(2-aminoethyl) amine moiety, $T = 25$, 35, 45, and 55 °C, dosage = 2 g L^{-1}, 80 rpm, and $C_i = 10$ mg L^{-1}, $t = 5$ min, $pH_i = 7.0$)

with what has been recently published regarding the sorption of uranium(VI) ion from aqueous solutions by using amidoxime-silica [72]. This indicates the endothermic sorption reaction and capturing process. We notice that no highly significant effect of temperature has appeared. Therefore, from the economic view, we use $T = 25$ °C for all experiment batches.

Thermodynamic isotherm

The sorption isotherms is a function of the uranium (VI) ion amount adsorbed into the SG-TAEA-NH_2 surface. To investigate the distribution of uranium(VI) ion between the aqueous phase and the SG-TAEA-NH_2 solid phase, the adsorption data were analyzed by using the Langmuir [94] and the Freundlich [95] adsorption isotherms. The isotherm experiments were conducted by using 1, 5, 10, and 20 mg L^{-1} of UO_2^{2+} ion solutions. All other sorption parameters are kept constant for each experiment (e.g. $pH_i = 7$, $T = 25$ °C and 2 g L^{-1} dosage of SG-TAEA-NH_2 material.

The Langmuir isotherm model of the uniform monolayer adsorption onto a surface can be linearized as given by Eq. 7:

$$\frac{C_e}{q_e} = \frac{1}{q_{max} b} + \frac{1}{q_{max}} C_e \tag{7}$$

where q_{max} is the adsorption capacity and the maximum capturing of uranium (VI) ion per unit dosage of SG-TAEA-NH_2 material (mg g^{-1}); and the energy of adsorption b is Langmuir constant (L g^{-1}), which is exponentially proportional to the heat of adsorption and the affinity of binding sites. The linear plot of (C_e/q_e) versus the equilibrium concentration (C_e) gives a straight line. The slope of the plot gives $\frac{1}{q_{max}}$, while the intercept of the plot gives $\frac{1}{q_{max} b}$.

The Freundlich model represents the heterogeneous sorption of U(VI) ion on the surface of SG-TAEA-NH_2 material followed by a condensation effect resulting from strong U(VI)-U(VI) ions interaction. The linear form of the Freundlich model is also given by Eq. 8:

$$\ln q_e = \ln K_F + \left(\frac{1}{n}\right) \ln C_e \tag{8}$$

Where qe represents the amount adsorbed U(VI) ion per amount of SG-TAEA-NH_2 material at the equilibrium (mg g^{-1}), Ce represents the equilibrium concentration (mg L^{-1}), K_f (mg g^{-1}) and n is the sorption capacity of the SG-TAEA-NH_2 material and the intensity of sorption, respectively. The plot of the ln q_e versus ln C_e gives the slope ($=\frac{1}{n}$) and intercept ($=\ln K_f$). The higher $\frac{1}{n}$ the value indicates the more favorable of the chemisorption. The Freundlich adsorption correlation coefficients (R^2), K_f and n are presented in Table 1.

Table 1 Freundlich constants of K_f and n

T (°C)	n	K_f	R^2
25	0.49766	45.7641	0.9999
35	1.05274	21.1640	0.9947
45	0.31931	65.1635	0.9963
55	0.46034	55.4954	0.9987

Figures 5 and 6 exhibit Freundlich and Langmuir plots, respectively, for the sorption of U(VI) cation into the SG-TAEA-NH_2 surface. The Langmuir sorption isotherm gives $R^2 < 0.800$, which measure a bad goodness-of-fit for the experimental results. While the results reveal that the Freundlich sorption isotherm is the best model ($R^2 > 0.99$). From the chemical point of view regarding the behavior of the complex reaction system on the surface, it should behave like a monolayer behavior following the Langmuir sorption isotherm model. Nevertheless, what we found is the opposite. The suggestion reason is that the SG-TAEA-NH_2 surface does not have complete coverage by TAEA-NH_2 entities. With this visualization, there is a small part of (≡Si−O–H) on the surface of silica gel still active, wherein most of the surface is covered with TAEA-NH_2 entities. Through the sorption process, part of the U(VI) ion is adsorbed by ≡Si−O–H entities and other bulk ions captured by TAEA-NH_2 entities. For this, we find that adsorption is heterogeneous and follows Freundlich sorption isotherm. Nearly similar results have been reported [85, 96]. Wherein, the heterogeneous layer of uranium (VI) ion is formed on the surface of powdery aerobic activated sludge including carboxyl (−COOH), Hydroxyl (−OH), Amino (−NH_2) achieving Freundlich isotherm [96]. Besides, our results are not in good qualitatively agreement with those found from adsorption of the iron ion with the SG-TAEA-NH_2 material [85]. The reason may be due to the interaction affinity of iron and uranium with SG-TAEA-NH_2 material and ≡Si−O–H entities in the acidic and neutral medium, respectively.

The thermal parameters ΔH and ΔS can be calculated by using Vant Hoff linear Eq. 9:

$$\ln k_c = \frac{\Delta S^o}{R} - \frac{\Delta H^o}{RT} \tag{9}$$

The linear plot of the Vant-Hoff ($\ln k_c$ vs $\frac{1}{T}$) gives the slope $= \frac{H^o}{R}$ and the intercept $= \frac{S^o}{R}$ (see Fig. 7 and Table 2).

The positive value of enthalpy change ($\Delta H = +48.71422$ kJ mol^{-1}) suggests the possibility of a strong binding between the UO_2^{2+} ion and the active site on the surface of the SG-TAEA-NH_2 as an endothermic process. That means, the positive value of ΔH° further confirms the endothermic nature of the sorption. The positive value of entropy change ($\Delta S = +0.1846623$ kJ mol^{-1} K^{-1})

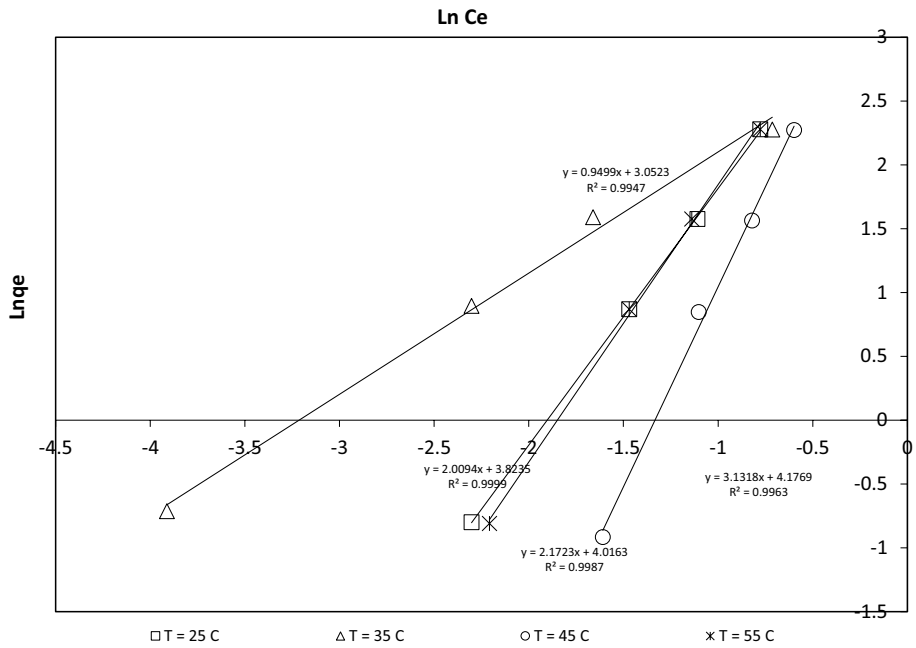

Fig. 5 Frunedlich isotherm on the sorption of uranium (VI) ion by using Silica Gel particles functionalized tris(2-aminoethyl)amine moiety $T = 25$, 35, 45, and 55 °C, dosage = 2 g L^{-1}, 80 rpm, and $C_i = 1$, 5, 10, and 20 mg L^{-1}, $t = 10$ min, pH = 7.0

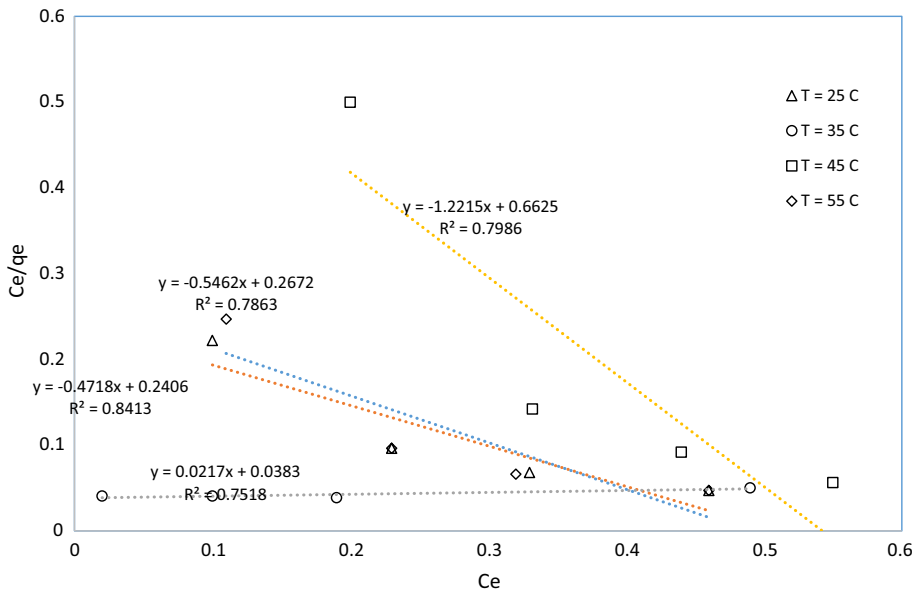

Fig. 6 Langmuir isotherm on the capture of uranium (VI) ion from water by using Silica Gel functionalized tris(2-aminoethyl)amine moiety, $T = 25$, 35, 45, and 55 °C, dosage = 2 g L^{-1}, 80 rpm, and $C_i = 1$, 5, 10, and 20 mg L^{-1}, $t = 10$ min, pH = 7.0

reflects a good affinity of uranium (VI) ion towards the SG-TAEA-NH_2 surface and increases the randomness at the solid–liquid interface during the sorption. At high temperature, the water molecules surrounded uranium (VI) ion decrease; this leads to increase the water molecules freedom. From other directions, less positive ΔS is due to the decreasing number of free molecules to add in on particle molecule of SG-TAEA-NH_2-U^{6+}, they were two fragments and be one fragment.

The spontaneity of sorption can be measured by the Gibbs free energy (ΔG). Based on obtaining isotherm results, the best choice to calculate ΔG is Eq. 10:

$$G = \Delta H - T\Delta S \tag{10}$$

The calculated ΔG are found to be a negative in sign ($\Delta G < 0$) based on the changing in temperature values (25, 35, 45, and 55 °C, see Table 2). This indicates the spontaneous interaction of uranium ion into the SG-TAEA-NH_2 surface as shown in Fig. 8. Furthermore, $\Delta G°$ values are

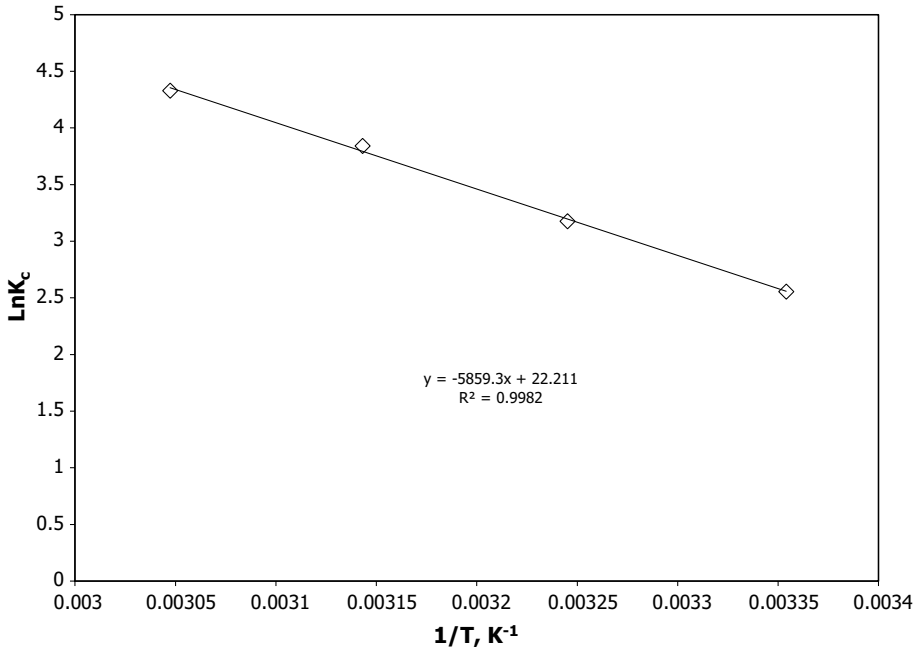

Fig. 7 The plot of ln K_c versus I/T regarding the capturing of uranium (VI) ion by using Silica Gel particles functionalized tris(2-aminoethyl)amine moiety, $t = 2$ min, dosage = 2 g L^{-1}, 80 rpm, and $C_i = 10$ mg L^{-1}, pH = 7.0

Table 2 Thermodynamic parameters of capturing U(VI) ion by SG-TAEA-NH_2 material

T (C)	ΔG (kJ mol^{-1})	ΔH (kJ mol^{-1})	ΔS (kJ mol^{-1} K^{-1})
25	−63.4283	+48.71422	+0.1846623
35	−81.8945		
45	−100.361		
55	−118.827		

found more negative and higher than −40 kJ/mol, which indicates a chemisorption process.

The DKR isotherm is reported to be more general than the Langmuir and Freundlich isotherms. It helps to determine the apparent energy of adsorption. The characteristic porosity of adsorbent toward the adsorbate and does not assume a homogenous surface or constant sorption potential [97]. The Dubinin–Kaganer–Radushkevich (DKR) model has the linear form as in Eq. 11:

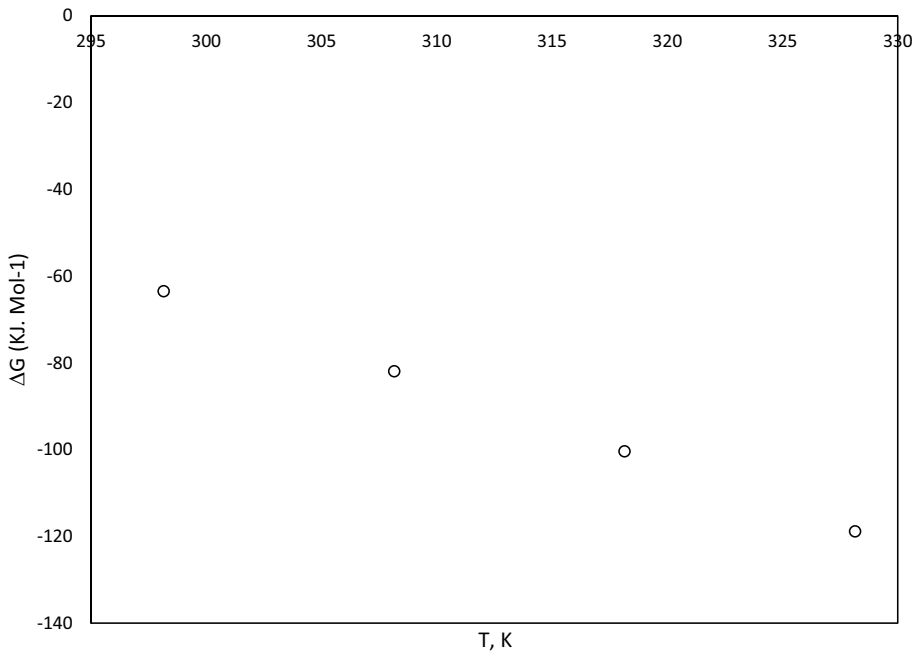

Fig. 8 Plot of The value of standard Gibbs free energy change (G) versus temperatures ($T = 25$, 35, 45, and 55 °C) for capturing of uranium (VI) ion from water by using the SG-TAEA-NH_2

$$\ln q_e = \ln q_{max} - \beta\varepsilon^2 \quad (11)$$

wherein q_e is DKR monolayer capacity (mg g^{-1}), β is adsorption energy constant, q_{max} is the amount of U(VI) ion adsorbed per unit weight of SG-TAEA-NH_2 material (mg g^{-1}), and ε is the Polanyi potential. The Polanyi potential can be calculated by using Eq. 12:

$$\varepsilon = RT \ln\left(1 + \frac{1}{C_e}\right) \quad (12)$$

wherein C_e is the equilibrium concentration of U(VI) ion in aqueous solution (mg L^{-1}), R is the gas constant, T is the temperature (K).

The sorption energy E can be calculated by Eq. 13:

$$E = -\frac{1}{\sqrt{-2\beta}} \quad (13)$$

wherein The Dubinin–Kaganer–Radushkevich sorption energy E can confirm the adsorption mechanism as follow [98]:

E (kJ mol^{-1})	Indication
−1 to −8	Physisorption
−8 to −16	Ion-exchange
−20 to −40	Chemisorption

The slope of the plot of $\ln q_e$ versus ε^2 gives β (mol^2 J^{-2}) and the intercept yields the sorption capacity, q_{max} as shown in Fig. 9. The values of β and E, as a function of temperature, are listed in Table 3 with their corresponding value of the correlation coefficient, R^2. The E value obtained shows that the sorption follows the chemisorption mechanism.

Table 3 Dubinin–Kaganer–Radushkevich sorption parameters

T	β	E	R^2
25	−8.43	−24.3541	0.9809
35	−29.047	−13.12	0.9803
45	−3.7531	−36.4998	0.9945
55	−7.4985	−25.8225	0.9913

Adsorption kinetic

Effect of contact time

To study the kinetic models of such a sorption system, it is worth describing the sorption rate of aqueous U(VI) ion as a function of time-based (1) changing the initial concentration or (2) changing the Temperature.

Figure 10a–c show the effect of contact time onto the sorption process that controlled by changing initial concentration, temperatures, and pH_i. In all cases, we find that the removal rate of uranium (VI) ion is high in the first 5 min. This is due to the availability of the uncovered surface area of the SG-TAEA-NH_2 surface. During the next 5 min, the sorption equilibrium starts yielded a maximum removal of 99% (approx.). This finding is found better than what has been recently published regarding the removal of the U(IV)

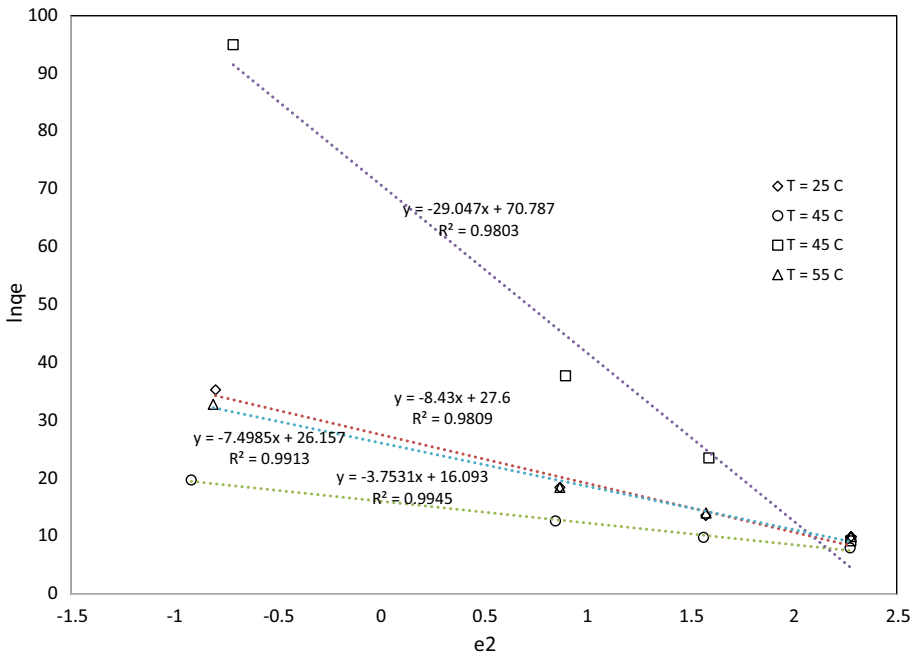

Fig. 9 Dubinin–Kaganer–Radushkevich isotherm on the capture of uranium (VI) ion from water by using Silica Gel particles functionalized tris(2-aminoethyl)amine moiety, T = 25, 35, 45, and 55 °C, dosage = 2 g L^{-1}, 80 rpm, and C_i = 1, 5, 10, and 20 mg L^{-1}, t = 10 min, pH = 7.0

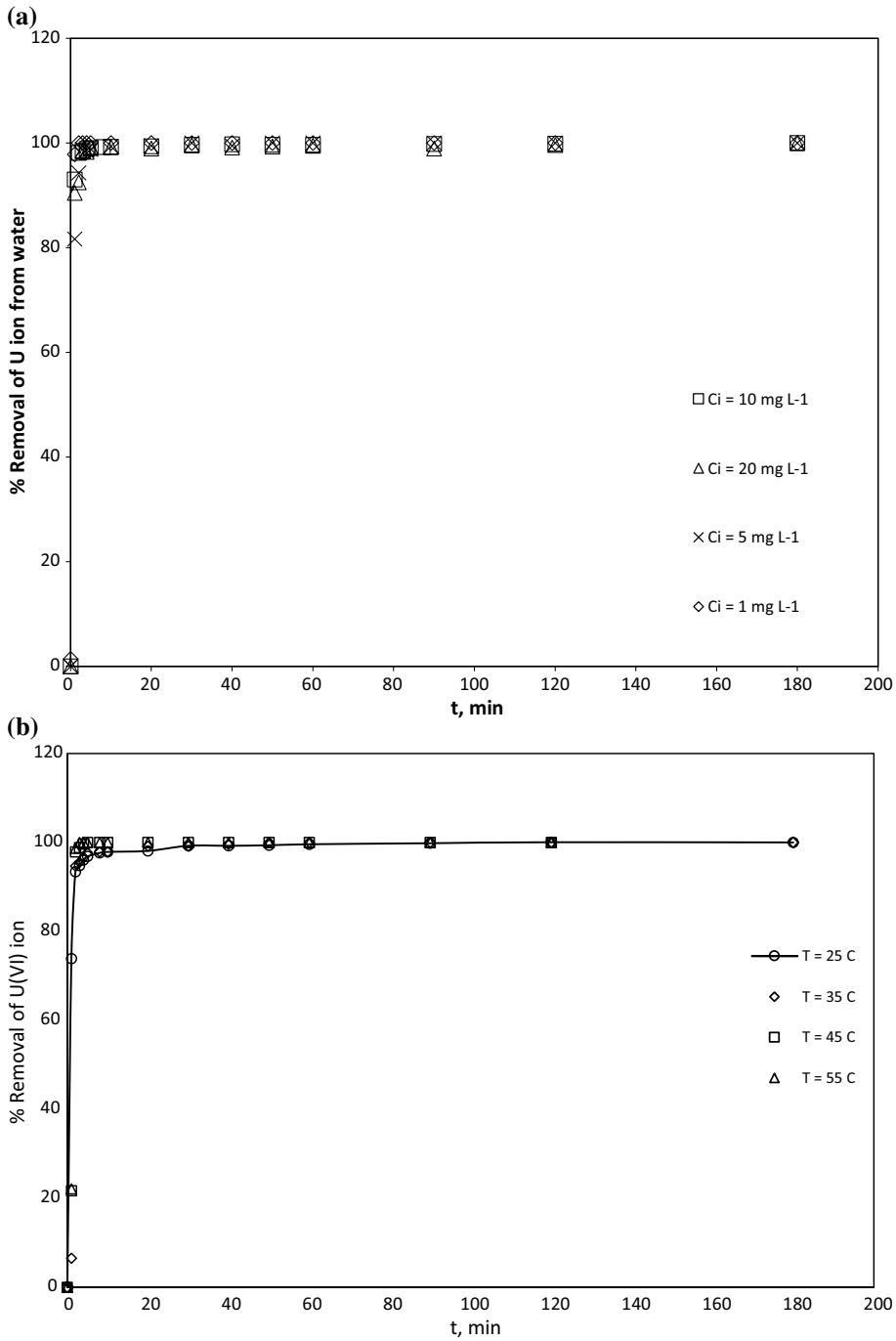

Fig. 10 **a** The effect of contact time controlled by changing initial concentration on the capture of uranium (VI) ion from water by using Silica Gel functionalized tris(2-aminoethyl)amine moiety ($T = 25$ °C, dosage = 2 g L^{-1}, 80 rpm, and $C_i = 20$, 10, 5, and 1 mg L^{-1}, pH = 7). **b** The effect of contact time controlled by changing temperatures on the capture of uranium (VI) ion from water by using Silica Gel functionalized tris(2-aminoethyl)amine moiety ($T = 25$, 35, 45, and 55 °C, dosage = 2 g L^{-1}, 80 rpm, and $C_i = 10$ mg L^{-1}, pH = 7). **c** The effect of contact time controlled by changing pH on the capture of uranium (VI) ion from water by using Silica Gel functionalized tris(2-aminoethyl) amine moiety ($T = 25$ °C, dosage = 2 g L^{-1}, 80 rpm, and $C_i = 10$ mg L^{-1})

ion by using an NH_2-functionalized ordered silica [99] and amidoxime silica [72].

Sorption kinetic model

The rate constant and rate-determining step of the reaction can be measured by using the sorption kinetic models. In this respect, two commonly kinetic models of the sorption are used. Wherein, the pseudo-first-order kinetic model and its integral can be expressed by Eq. 14 [100, 101]:

$$\ln(q_e - q_t) = \ln q_e - k_1 t \tag{14}$$

where q_e and q_t (mg g^{-1}) are the amounts of adsorbed U(VI) ion at equilibrium and at the time (t), respectively, k_1 (min^{-1}) is the pseudo-first-order rate constant, and t (min) is contact time. The linear plot of $\ln(q_e - q_t)$ versus t provides the slop of the k_1 and the intercept of $\ln q_e$.

Besides, the pseudo-second-order kinetic model and its integral form are expressed by Eq. 15 [102, 103]:

Fig. 10 (continued)

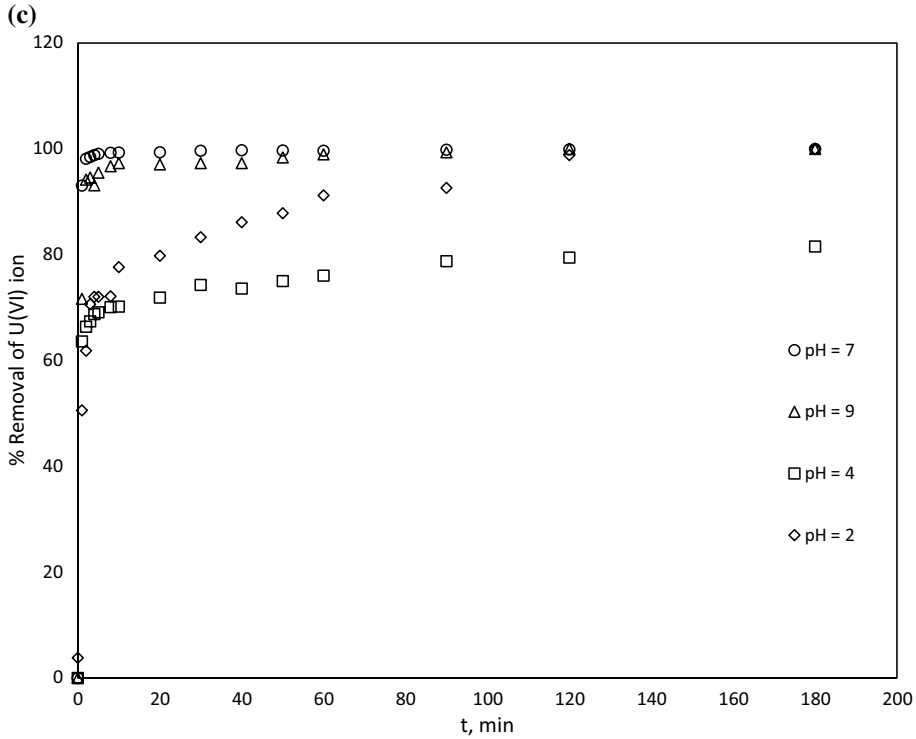

$$\frac{t}{q_t} = \frac{1}{k_2 q_e^2} + \frac{t}{q_e} \quad (15)$$

where k_2 is the rate constant of the pseudo-second-order kinetic model (g mg^{-1} min^{-1}). The value of k_2 and q_e can be determined from the intercept and slop that can be generated by a plot of $\frac{t}{q_t}$ versus t.

Firstly, the kinetics sorption describes the removal rate of aqueous U(VI) ion based on the changing of the initial concentration (C_i = 1, 5, 10, 20 mg L^{-1}) at constant other parameters (pH_i = 7, 80 rpm, dosage = 2 g L^{-1} of SG-TAEA-NH$_2$ surface and T = 25 °C). Figures 11 and 12 show the pseudo-second-order kinetic and pseudo-first-order kinetic models, respectively. The pseudo-first-order kinetic model has the coefficient of determination value (R^2), which is less than

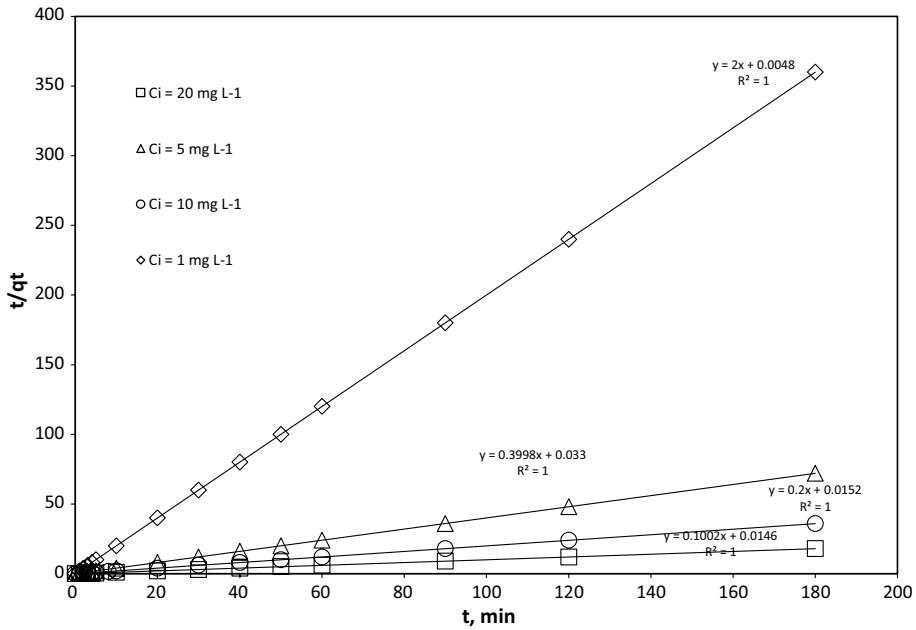

Fig. 11 Pseudo-second order model related to the capture of uranium (VI) ion from water by using Silica Gel functionalized tris(2-aminoethyl)amine moiety, T = 25 °C, dosage = 2 g L^{-1}, 80 rpm, and C_i = 20, 10, 5 mg L^{-1}, pH = 7.0

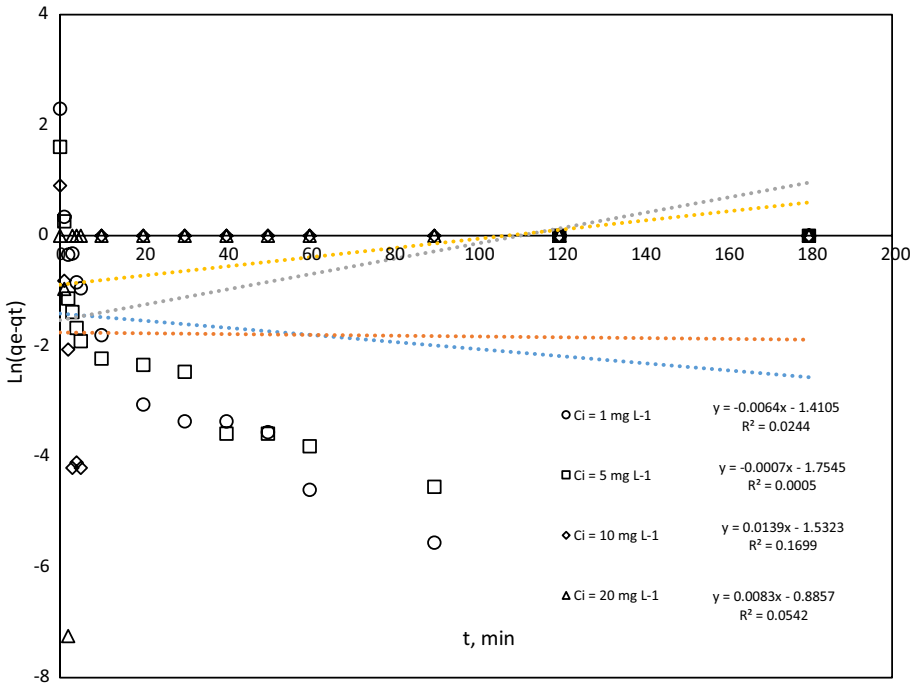

Fig. 12 Pseudo-first order model related to the capture of uranium (VI) ion from water by using Silica Gel functionalized tris(2-aminoethyl)amine moiety, $T = 25$ °C, dosage = 2 g L^{-1}, 80 rpm, and $C_i = 20$, 10, 5 mg L^{-1}, pH = 7.0

0.020. While, the pseudo-second-order kinetic model has a correlation coefficient $R^2 = 1.0$, which approve the results.

Secondly, the kinetic sorption describes the removal rate of aqueous U(VI) ion as a function of changing the temperatures ($T = 25$, 35, 45 and 55 °C) at constant other parameters ($pH_i = 7$, 80 rpm, dosage = 2 g L^{-1} of SG-TAEA-NH_2 surface and $C_i = 10$ mg L^{-1}). The pseudo-second-order kinetic model has a linear plot with $R^2 > 0.995$ as shown in Fig. 13. While the pseudo-first-order kinetic model has the coefficient of determination value $R^2 < 0.026$. Therefore, the kinetic adsorption data were satisfactorily fitted to the pseudo-second-order model.

Based on kinetic adsorption experiments as a function of changing the temperatures or initial concentration *vs.* contact time, the kinetic sorption data indicate that the pseudo-second-order kinetic model can perfectly describe the sorption

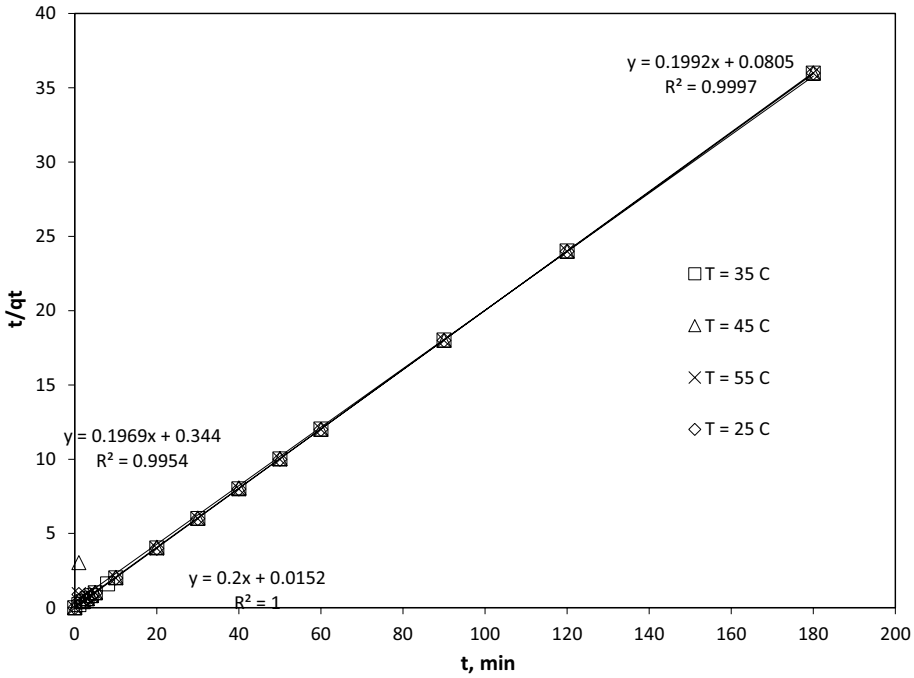

Fig. 13 Pseudo-second order model related to the capture of uranium (VI) ion from water by using Silica Gel functionalized tris(2-aminoethyl)amine moiety, $T = 25$, 35, 45 and 55 °C, dosage = 2 g L^{-1}, 80 rpm, and $C_i = 10$ mg L^{-1}, pH = 7.0

reaction of uranium ion onto SG-TAEA-NH_2 surface. This means that the U(VI) ion can be chemi-adsorbed by the sorption sites onto the SG-TAEA-NH_2 surface as shown in Schemes 2 and 3. We use tow experiment functions to be further proof that adsorption exhibits chemisorption behavior. The good matching between the experimental and the calculated (q_{exp} and q_{cal}) support the finding results of kinetic models as listed in Tables 4 and 5. This result was found matching with the reported one by utilizing amidoxime silica [72] and adsorbing iron by SG-TAEA-NH_2 material [85].

Figure 14 shows the plot of the *Arrhenius* equation ($\ln k_2$ versus $\frac{1}{T}$ as in Eq. 16), which gives the slop ($=-\frac{E_a}{R}$) and intercept ($\ln A$). Wherein, the E_a and A is the activation energy and collision frequency, respectively.

$$\ln k_2 = \ln A - \frac{E_a}{RT} \tag{16}$$

The calculated activation energy ($E_a = -192.144854$ kJ mol^{-1}) has a negative sign. In this case, it is possible. There are attractive forces between the amino groups in the surface and uranium ion, there are no barrier, or the barrier is submerged. This means that barrierless or there are complexes on the potential energy surfaces between the U(VI) ion and the surface of the adsorbent.

The Weber-Moris intraparticle diffusion model regarding the sorption of the U(VI) cation into the SG-TAEA-NH_2 surface can be discussed through the plot of the q_t *vs.* $\sqrt{t}$ as mention in Eq. 17 [104]:

$$q_t = k_{int}\sqrt{t} + C \tag{17}$$

wherein k_{int} is the intraparticle diffusion rate constant (mg g^{-1} min$^{\frac{1}{2}}$). The straight line of the plot confirms intraparticle diffusion sorption. A plot presents multi-linearity, which indicates that three steps occur. These are the external surface adsorption (0–2 min), intraparticle diffusion (3 up to 20 min), and final equilibrium stage ($t > 20$ min). Herein, we could say that the intraparticle diffusion could be the rate-controlled ($k_{int} = 0.0479$ mg g^{-1} min$^{\frac{1}{2}}$ and $R^2 = 0.8031$, see Fig. 15). This finding matches our recent study related to using SG-TAEA-NH_2 material for the sorption of iron ion from water [85].

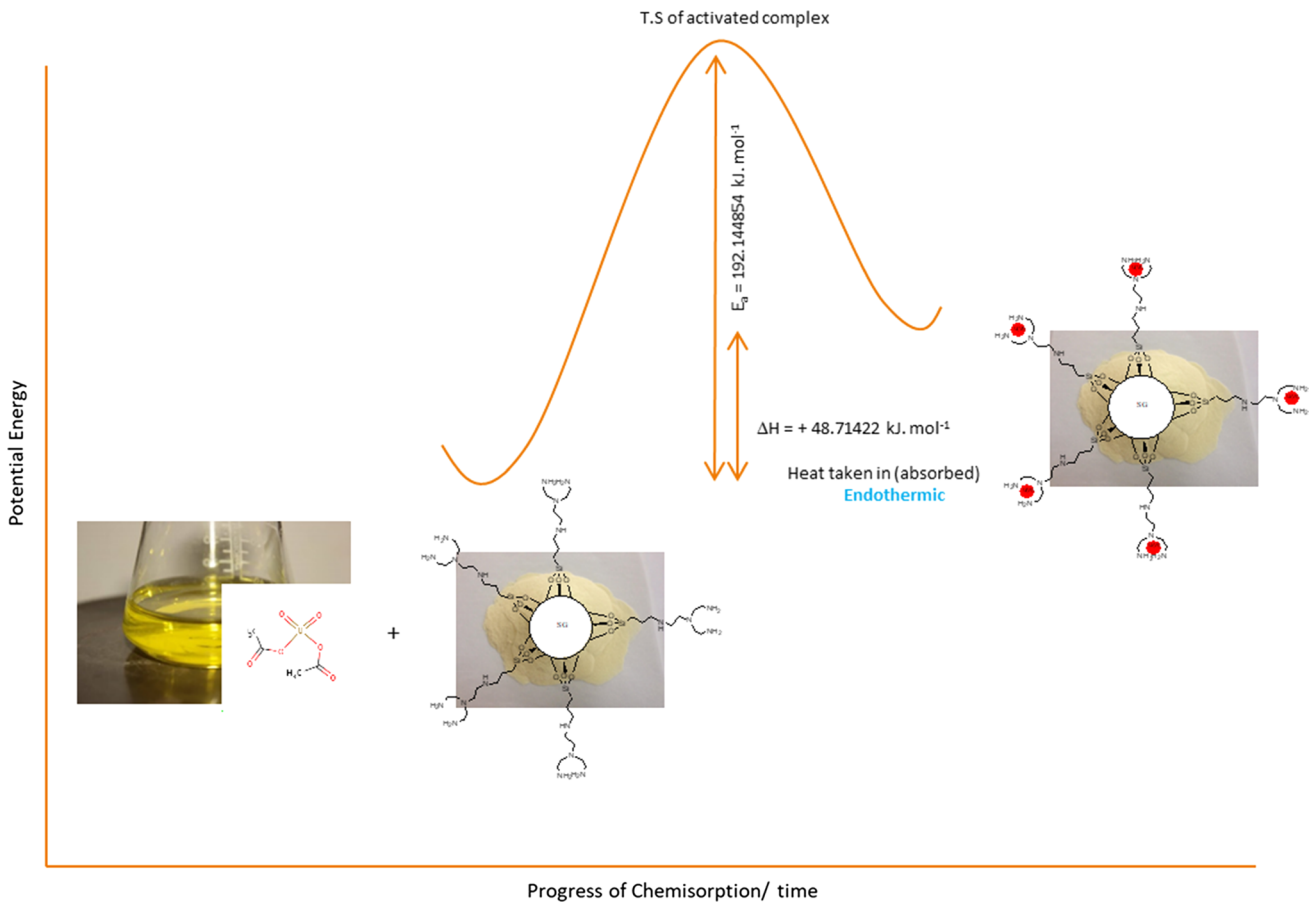

Scheme 2 Reaction progress of sorption uranium (VI) ion onto the SG-TAEA-NH_2 surface

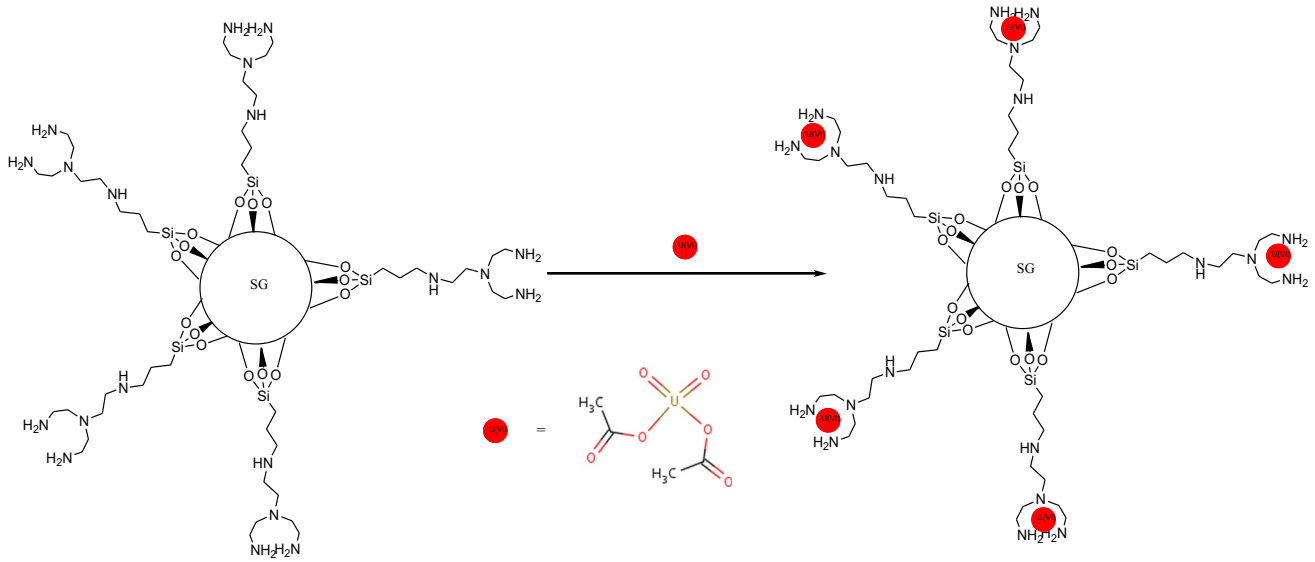

Scheme 3 Schematic representation of chemisorptions of U(VI) ion by the sorption sites of the SG-TAEA-NH_2 surface

Table 4 The parameters of the pseudo-Second order kinetic model

R^2	q_e, Calc (mg g^{-1})	q_e, Exp (mg g^{-1})	k_2 (g mg^{-1} min^{-1})	C_i = mg L^{-1}
1.00	0.490	0.500	833.3333	1
1.00	2.485	2.501	4.844608	5
1.00	4.999	5.000	2.631579	10
1.00	9.960	9.980	0.687679	20

Table 5 The parameters of the pseudo-second order kinetic model

R^2	$q_{e,\,Calc}$ (mg g^{-1})	$q_{e,\,Exp}$ (mg g^{-1})	k_2 (g mg^{-1} min^{-1})	T (°C)
1.0000	4.995	5.000	2.631579	25
0.9954	4.980	5.079	0.11269	35
0.9997	4.980	5.020	0.492943	45
		5.018	0.514506	55

Conclusion

Capturing of uranium (VI) ion from water by the silica gel functionalized tris(2-aminoethyl)amine moiety (SG-TAEA-NH_2) is effective in the pH range of 7–9. The capturing percentage increases by increasing the temperature and decreasing the initial concentration. The maximum capturing is 99% based on the sorption parameters of $T = 25$ °C, dosage = 2 g L^{-1}, 80 rpm, and low initial concentration, $t = 5$ min. The sorption equilibrium can be reached within 5–10 min in maximum. The obtained experimental data have excellent fits within the Freundlich isotherm ($R^2 > 0.999$) proving that the surface of SG-TAEA-NH_2 is un-uniform. The kinetic sorption data fits very well with the pseudo-second-order model indicating chemisorption behavior. Depending on the logic of coordination chemistry, sorption isotherm, FTIR, and kinetic model, the metal complex spheres can be formed spontaneous, favorable on the surface through the chemical interaction between the primary amine active sites (–NH_2) and U(VI) ion as heterogonous-layers. The new finding is the utilization of SG-TAEA-NH_2 as a good potential material for the removal of uranium ion from water.

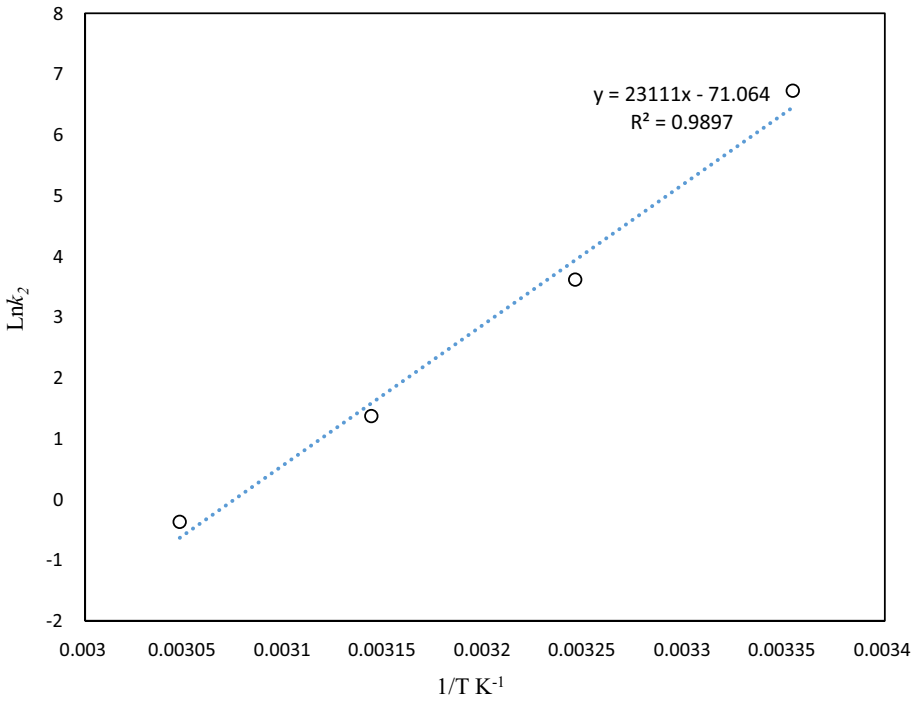

Fig. 14 The Arrhenius plot related to the capture of uranium (VI) ion from water by using Silica Gel functionalized tris(2-aminoethyl)amine moiety

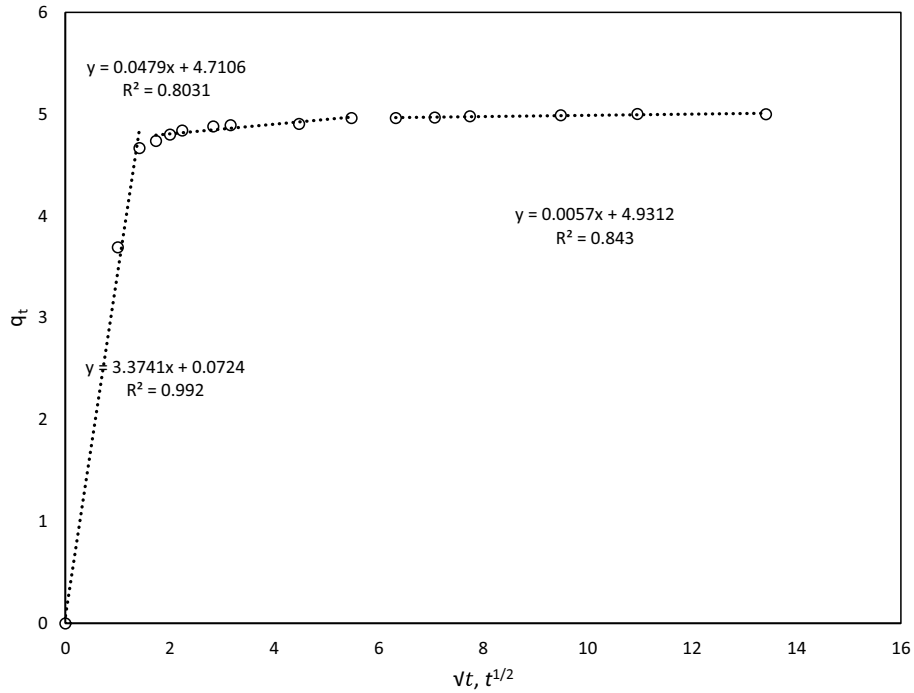

Fig. 15 Weber-Moris intraparticular diffusion model related to the capture of uranium (VI) ion from water by using Silica Gel functionalized tris(2-aminoethyl)amine moiety, $T = 25$ °C, dosage = 2 g L^{-1}, 80 rpm, and $C_i = 10$ mg L^{-1}, pH = 7.0

References

1. Shao DD, Hou GS, Li JX, Ren XM, Wang XK (2014) PANI/GO as a super adsorbent for the selective adsorption of uranium(VI). Chem Eng J 255:604–612
2. Fiedor JN, Bostick WD, Jarabek RJ, Farrell J (1998) Understanding the mechanism of uranium removal from groundwater by zero-valent iron using X-ray photoelectron spectroscopy. Environ Sci Technol 32:1466–1473
3. Kim I-G, Kim S-S, Kim G-N, Han G-S, Choi J-W (2016) Reduction of radioactive waste from remediation of uranium-contaminated soil. Nucl Eng Technol 48:840–846
4. Ebbs SD, Norvell WA, Kochian LV (1998) The effect of acidification and chelating agents on the solubilization of uranium from contaminated soil. J Environ Qual 27:1486–1494

5. Grenthe I, Fuger J, Konings RJM, Lemire RJ, Muller AB, Nguyen-Trung C, Wanner H (1992) Chemical thermodynamics of uranium. Elsevier, New York, p 715
6. Shen GT, Dunbar RB (1995) Environmental controls on uranium in reef corals. Geochim Cosmochim Acta 59:2009–2024
7. Ulrich K-U, Veeramani H, Bernier-Latmani R, Giammar DE (2011) Speciation-dependent kinetics of uranium(VI) bioreduction. Geomicrobiol J 28:396–409
8. Bühl M, Kabrede H (2006) Mechanism of water exchange in aqueous uranyl(VI) ion. A density functional molecular dynamics study. Inorg Chem 45:3834–3836
9. Domingo JL (2001) Reproductive and developmental toxicity of natural and depleted uranium: a review. Reprod Toxicol 15:603–609
10. Memon JR, Hallam KR, Bhanger MI, Turki AE, Allen GC (2009) Evaluation of sorption of uranium onto metakaolin using X-ray photoelectron and Raman spectroscopies. Anal Chim Acta 631(1):69–73
11. David Van Horn J, Huang H (2006) Uranium(VI) bio-coordination chemistry from biochemical, solution, and protein structural data. Coord Chem Rev 250:765–775
12. Karve M, Rajgor RV (2008) Amberlite XAD-2 impregnated organophosphinic acid extractant for separation of uranium(VI) from rare earth elements. Desalination 232:191–197
13. Kilislioglu A, Bilgin B (2003) Thermodynamic and kinetic investigations of uranium adsorption on amberlite IR-118H resin. Appl Radiat Isot 58:155–160
14. Rahmati A, Ghaemi A, Samadfam M (2012) Kinetic and thermodynamic studies of uranium(VI) adsorption using Amberlite IRA-910 resin. Ann Nucl Energy 39:42–48
15. Kuhu AT (1972) Electrochemistry of cleaner environments. Plenum Press, New York
16. Elsayed HM, Fouad EA, El-Hazek NMT, Khoniem AK (2013) Uranium extraction enhancement from phosphoric acid by emulsion liquid membrane. J Radioanal Nucl Chem 298:1763–1775
17. Gafvert T, Ellmark C, Holm E (2002) Removal of radionuclides at a waterworks. J Environ Radioact 63:105–115
18. Lee SY, Bondietti EA (1983) Removing uranium from drinking water by metal hydroxides and anion-exchange resin. J Am Water Works Assoc 75:536–540
19. Ohashi Y, Harada M, Asanuma N, Ikeda Y (2015) Feasibility studies on electrochemical recovery of uranium from solid wastes contaminated with uranium using 1-butyl-3-methylimidazorium chloride as an electrolyte. J Nucl Mater 464:119–127
20. Poirier RH, Calkins GD, Lutz GA, Bearse AE (1958) Ion exchange separation of uranium from thorium. Ind Eng Chem 50:613–616
21. Rafati L, Mahvi AH, Asgari AR, Hosseini SS (2010) Removal of chromium (VI) from aqueous solutions using Lewatit FO36 nano ion exchange resin. Int J Environ Sci Technol 7:147–156
22. Asai S, Limbeck A (2015) LA-ICP-MS of rare earth elements concentrated in cation-exchange resin particles for origin attribution of uranium ore concentrate. Talanta 135:41–49
23. Djedidi Z, Bouda M, Souissi MA, Ben CR, Mercier G, Tyagi RD, Blais JF (2009) Metals removal from the soil, fly ash and sewage sludge leachates by precipitation and dewatering properties of the generated sludge. J Hazard Mater 172:1372–1382
24. Huxstep MR and Sorg TJ (1988) Removal of inorganic contaminants by reverse osmosis pilot plants. Project summary EPA/600/S2–87/109, U.S E.P.A., Cincinnati, OH
25. Cojocaru C, Zakrzewska-Trznadel G, Jaworska A (2009) Removal of cobalt ions from aqueous solutions by polymer assisted ultrafiltration using an experimental design approach. Part 1: optimization of complexation conditions. J Hazard Mater 169:599–609
26. Kedari CS, Pandit SS, Gandhi PM (2013) Separation by competitive transport of uranium(VI) and thorium(IV) nitrates across supported renewable liquid membrane containing trioctylphosphine oxide as a metal carrier. J Membr Sci 430:188–195
27. Rao TP, Metilda P, Gladis JM (2006) Preconcentration techniques for uranium (VI) and thorium (IV) prior to analytical determination—an overview. Talanta 68:1047–1064
28. Dietz ML, Horwitz EP, Sajdak LR, Chiarizia R (2001) An improved extraction chromatographic resin for the separation of uranium from acidic nitrate media. Talanta 54:1173–1184
29. Aldrich C, Feng D (2000) Removal of heavy metals from wastewater effluents by biosorptive flotation. Miner Eng 13:1129–1138
30. Kausar A, Bhatti H (2013) Adsorptive removal of uranium from wastewater: a review. J Chem Soc Pak 35(3):1041–1052
31. Zhang W, Ye G, Chen J (2013) Novel mesoporous silicas bearing phosphine oxide ligands with different alkyl chains for the binding of uranium in strong HNO_3. Media J Mater Chem A 1:12706–12709
32. Yuan L-Y, Liu Y-L, Shi W-Q, Lv Y-L, Lan J-H, Zhao Y-L, Chai Z-F (2011) High performance of phosphonate-functionalized mesoporous silica for U(vi) sorption from aqueous solution. Dalton Trans 40:7446–7453
33. Nogami M, Ishihara T, Maruyama K, Ikeda Y (2008) Effect of chemical structure of monoamide resins on adsorptivity to uranium(VI) in nitric acid media. Prog Nucl Energy 50:462–465
34. Zhang S, Zhao XS, Li B, Bai CY, Li Y, Wang L, Wen R, Zhang MC, Ma LJ, Li SJ (2016) Stereoscopic 2D super-microporous phosphazene-based covalent organic framework: design, synthesis and selective sorption towards uranium at high acidic condition. J Hazard Mater 314:95–104
35. Motawie AM, Mahmoud KF, El-Sawy AA, Kamal HM, Hefni H, Ibrahiem HA (2014) Preparation of chitosan from the shrimp shells and its application for pre-concentration of uranium after cross-linking with epichlorohydrin. Egypt J Petrol 23:221–228
36. Wang G, Liu J, Wang X, Xie Z, Deng N (2009) Adsorption of uranium (VI) from aqueous solution onto cross-linked chitosan. J Hazard Mater 168:1053–1058
37. Abdi S, Nasiri M, Mesbahi A, Khani MH (2017) Investigation of uranium (VI) adsorption by polypyrrole. J Hazard Mater 332:132–139
38. Akyil S, Eral M (2005) Preparation of composite adsorbents and their characteristics. J Radioanal Nucl Chem 266:89–93
39. Mahmoud MA (2018) Adsorption of U(VI) ions from aqueous solution using silicon dioxide nanopowder. J Saud Chem Soc 22:229–238
40. Yu J, Bai H, Wang J, Li Z, Jiao C, Liu Q, Zhang M, Liuc L (2013) Synthesis of alumina nanosheets via supercritical fluid technology with high uranyl adsorptive capacity. New J Chem 37:366–372
41. Yang D, Zheng ZF, Zhu HY, Liu HW, Gao XP (2008) Titanate nanofibers as intelligent absorbents for the removal of radioactive ions from water. Adv Mater 20:2777–2781
42. Barber PS, Griggs CS, Rogers RD, Kelley SP, Wallace S (2014) Surface modification of ionic liquid-spun chitin fibers for the extraction of uranium from seawater: seeking the strength of chitin and the chemical functionality of chitosan. Green Chem 4:1828–1836
43. Saini AS, Melo JS (2013) Biosorption of uranium by melanin: kinetic, equilibrium, and thermodynamic studies. Bioresour Technol 149:155–162
44. Yi Z-j, Yao J, Zhu M-j, Chen H-l, Wang F, Liu X (2017) Uranium biosorption from aqueous solution by the submerged aquatic plant Hydrilla verticillata. Water Sci Technol 75(5–6):1332–1341
45. Simon FG, Biermann V, Peplinski B (2008) Uranium removal from groundwater using hydroxyapatite. Appl Geochem 23(8):2137–2145

46. Popa K (2013) Sorption of uranium on lead hydroxyapatite. J Radioanal Nucl Chem 298:1527–1532
47. El-Sayed AA (2008) Kinetics and thermodynamics of adsorption of trace amount of uranium on activated carbon. Radiochim Acta 96:481–486
48. Mellah A, Chegrouche S, Barkat M (2006) The removal of uranium(VI) from aqueous solutions onto activated carbon: kinetic and thermodynamic investigations. J Colloid Interface Sci 296:434–441
49. Kutahyalı C, Eral M (2004) Selective adsorption of uranium from aqueous solutions using activated carbon prepared from charcoal by chemical activation. Sep Purif Technol 40:109–114
50. Schierz A, Za¨nker H (2009) Aqueous suspensions of carbon nanotubes: surface oxidation, colloidal stability, and uranium sorption. Environ Pollut 157:1088–1094
51. Liu S, Li S, Zhang H, Wu L, Sun L, Ma J (2016) Removal of uranium(VI) from aqueous solution using graphene oxide and its amine-functionalized composite. J Radioanal Nucl Chem 309:607–614
52. Noubactep C, Schoner A, Meinrath G (2006) Mechanism of uranium removal from the aqueous solution by elemental iron. J Hazard Mater 132:202–212
53. Dickinson M, Scott TB (2010) The application of zero-valent iron nanoparticles for the remediation of uranium-contaminated waste effluent. J Hazard Mater 178:171–179
54. Zhang L, Huang L, Zeng Z, Qiana J, Hua D (2016) Zeta potential-assisted sorption of uranyl tricarbonate complex from aqueous solution by polyamidoxime-functionalized colloidal particles. Phys Chem Chem Phys 18:13026–13032
55. Wei K, Wang Q, Huang L, Sun L (2016) Amino-functionalized urea-formaldehyde framework mesoporous silica for U(VI) adsorption in wastewater treatment. Ind Eng Chem Res 55(48):12420–12429
56. Veliscek-Carolan J, Jolliffe KA, Hanley TL (2013) Selective sorption of actinides by titania nanoparticles covalently functionalized with simple organic ligands. ACS Appl Mater Interfaces 5(22):11984–11994
57. Wen T, Wang X, Wang J, Chen Z, Li J, Hu J, Hayat T, Alsaedi A, Grambow B, Wang X (2016) A strategically designed porous magnetic N-doped Fe/Fe_3C at C matrix and its highly efficient uranium(VI) remediation. Inorg Chem Front 3:1227–1235
58. Hsi C-KD, Langmuir D (1985) Adsorption of uranyl onto ferric oxyhydroxides: application of the surface complexation site-binding model. Geochim Cosmochim Acta 49:1931–1941
59. Waite TD, Davis JA, Payne TE, Waychunas GA, Xu N (1994) Uranium(VI) adsorption to ferrihydrite: application of a surface complexation model. Geochim Cosmochim Acta 58:5465–5478
60. Shuibo X, Chun Z, Xinghuo Z, Jing Y, Xiaojian Z, Jingsong W (2009) Removal of uranium (VI) from aqueous solution by adsorption of hematite. J Environ Radioact 100:162–166
61. Katsoyiannis IA (2007) Carbonate effects and pH-dependence of uranium sorption onto bacteriogenic iron oxides: kinetic and equilibrium studies. J Hazard Mater 139:31–37
62. Lefèvre G (2006) Study of uranyl sorption onto hematite by in situ attenuated total reflection–infrared spectroscopy. J Colloid Interf Sci 296:608–613. http://0j10241sz.y.https.www.sciencedirect.com.mu.proxy.coe-elibrary.com/science/article/pii/S0021979705009501. http://0j10241sz.y.https.www.sciencedirect.com.mu.proxy.coe-elibrary.com/science/article/pii/S0021979705009501
63. Tan L, Wang J, Liu Q, Sun Y, Zhang H, Wang Y (2015) Facile preparation of oxine functionalized magnetic Fe_3O_4 particles for enhanced uranium (VI) adsorption. Colloid Surf A Physicochem Eng Asp 466: 85–91. http://0j10241sz.y.https.www.sciencedirect.com.mu.proxy.coe-elibrary.com/science/article/pii/S0927775714008681. http://0j10241sz.y.https.www.sciencedirect.com.mu.proxy.coe-elibrary.com/science/article/pii/S0927775714008681
64. Pablo J, Duro L, Giménez J, Havel J, Torrero ME, Casas I (1992) Fluorimetric determination of traces of uranium(VI) in brines and iron(III) oxides using separation on an activated silica gel column. Anal Chim Acta 264:115–119
65. Abd El-Magied MO, Dhmees AS, Abd El-Hamid AM (2018) Uranium extraction by sulfonated mesoporous silica derived from blast furnace slag. J Nucl Mater 509:295–304. https://www.sciencedirect.com/science/article/pii/S0022311518300400
66. Chisholm-Brause C, Conradson SD, Buscher CT, Eller PG, Morris DE (1994) Speciation of uranyl sorbed at multiple binding sites on montmorillonite. Geochimica Cosmochim Acta 58:3625–3631
67. El-Shahat MF, Moawed EA, Farag AB (2007) Chemical enrichment and separation of uranyl ions in aqueous media using novel polyurethane foam chemically grafted with different basic dyestuff sorbents. Talanta 71:236–241
68. Han R, Wang Y (2007) Removal of uranium(VI) from aqueous solutions by manganese oxide coated zeolite: discussion of adsorption isotherms and pH effect. J Environ Radioact 93: 127–143. https://www.sciencedirect.com/science/article/pii/S0265931X06002128
69. James D, Venkateswaran G, Rao TP (2009) Removal of uranium from mining industry feed simulant solutions using trapped amidoxime functionality within a mesoporous imprinted polymer material. Microporous Mesoporous Mater 119:165–170
70. Yusan S, Aslani MAA, Turkozu DA, Aycan HA, Aytas S, Akyil S (2010) Adsorption and thermodynamic behavior of U(VI) on the *Tendurek volcanic* tuff. J Radioanal Nucl Chem 283:1–238
71. Wang J, Zhuang S (2019) Extraction and adsorption of U(VI) from aqueous solution using affinity ligand-based technologies: an overview. Rev Environ Sci Biotechnol 18:437–452
72. Yin X, Bai J, Fan F, Cheng W, Tian W, Wang Y, Qin Z (2015) Amidoximed silica for uranium(VI) sorption from aqueous solution. J Radioanal Nucl Chem 303:2135–2142
73. Michard P, Guibal E, Vincent T, Le Cloirec P (1996) Sorption and desorption of uranyl ions by silica gel: pH, particle size, and porosity effects. Micropor Mater 5:309–324
74. Tripathi S, Roy A, Nair S, Durani S, Bose R (2018) Removal of U(VI) from aqueous solution by adsorption onto synthesized silica and zinc silicate nanotubes: equilibrium and kinetic aspects with application to real samples. Environ Nanotechnol Monit Manag 10:127–139
75. Lerner N, Meyerstein D, Shamir D, Marks V, Shamish Z, Ohaion-Raz T, Maimon E (2019) A chemically modified silica-gel as an ion exchange resin for pre-concentration of actinides and lanthanides. Inorg Chim Acta 486:642–647
76. Donia AM, Atia AA, Desouky OA (2011) Selective separation of U(VI) from its solutions using amine-modified silica gel produced from leached zircon. Intern J Miner Process 101: 81–88. http://0j10241sz.y.https.www.sciencedirect.com.mu.proxy.coe-elibrary.com/science/article/abs/pii/S0301751611001050
77. Sadeghi S, Sheikhzadeh E (2009) Solid-phase extraction using silica gel modified with murexide for preconcentration of uranium (VI) ions from water samples. J Hazard Mater 163:861–868
78. Guibal E, Lorenzelli R, Vincent T, Cloirec PL (1995) Application of silica gel to metal ion sorption: static and dynamic removal of uranyl ions. Environ Technol 16:101–114
79. Barbette F, Rascalou F, Chollet H, Babouhot JL, Denat F, Guilard R (2004) Extraction of uranyl ions from aqueous solutions using silica-gel-bound macrocycles for alpha contaminated wastewater treatment. Anal Chim Acta 502:179–187
80. Mahmoud ME, Kenawy IMM, Soliman EM, Hafez MA, Akl MAA, Lashein RRA (2008) Selective preconcentration of uranyl

ion by silica gel phases modified with chelating compounds as inorganic polymeric ion exchangers. Anal Sci 24:381–387
81. Hasegawa H, Rahman I, Begum Z, Umehara Y, Maki T, Furusho Y, Mizutani S (2013) A silica gel-bound macrocycle system for the selective separation of toxic cadmium from the metal-affluent aqueous matrix. Cent Eur J Chem 11(3):341–347
82. Jung Y, Kim S, Jin S, Ji P, Kim M (2008) Application of polymer-modified nanoporous silica to adsorbents of uranyl ions. Colloids Surf A Physicochem Eng Asp 313:162–166
83. Venkatesan KA, Sukumaran V, Antony MP, Vasudeva Rao PR (2004) Extraction of uranium by an amine, amide, and benzamide grafted covalently on silica gel. J Radioanalyt Nucl Chem 260:443–450
84. Huang X, Chang X, He Q, Cui Y, Zhai Y, Jiang N (2008) Tris(2-aminoethyl) amine-functionalized silica gel for solid-phase extraction and preconcentration of Cr(III), Cd(II) and Pb(II) from waters. J Hazard Mater 157(1):154–160
85. Zaitoun MA, Al-Anber MA, Al Momani IF (2019) Sorption and removal aqueous iron(III) ion by tris(2-aminoethyl)amine moiety functionalized silica gel. Int J Environ Anal Chem. https://doi.org/10.1080/03067319.2019.1654466
86. Khan MH, Warwick P, Evans N (2006) Spectrophotometric determination of uranium with arsenazo-III in perchloric acid. Chemosphere 63(7):1165–9169
87. Arica TA, Ayas E, Arica MY (2017) Magnetic MCM-41 silica particles grafted with poly(glycidylmethacrylate) brush: modification and application for removal of direct dyes. Microporous Mesoporous Mater 243:164–175
88. Ladshaw AP, Wiechert AI, Das S, Yiacoumi S, Tsouris C (2017) Amidoxime polymers for uranium adsorption: influence of comonomers and temperature. Materials 10:1268
89. Liu Q, Zhu J, Tan L, Jing X, Liu J, Song D, Zhang H, Li R, Emelchenko GA, Wang J (2016) Polypyrrole/cobalt ferrite/multiwalled carbon nanotubes as an adsorbent for removing uranium ions from aqueous solutions. Dalton Trans 45:9166–9173
90. Satpati SK, Pal S, Goswami D, Tewari PK, Roy SB (2015) Extraction of uranium from nuclear industrial effluent using polyacrylhydroxamic acid sorbent. Int J Environ Sci Technol 12:255
91. Sepehrian H, Samadfam M, Asadi Z (2012) Studies on the recovery of uranium from nuclear industrial effluent using nanoporous silica adsorbent. Int J Environ Sci Technol 9:629–636
92. Cornelis R, Caruso J, Crews H, Heumann KG (2005) Handbook of elemental speciation II-species in the environment, food, medicine, and occupational health. Wiley, New York, pp 522–533
93. Bagherifam S, Lakzian A, Ahmadi SJ, Rahimi MF, Halajnia A (2010) Uranium removal from aqueous solutions by wood powder and wheat straw. J Radioanal Nucl Chem 283:289–296
94. Langmuir I (1918) The adsorption of gases on plane surfaces of glass, mica, and platinum. J Am Chem Soc 40:1361–1403
95. Freundlich HMF (1906) Z Phys Chem (Leipzig) 57A:385
96. Wang XL, Li Y, Huang J, Zhou YZ, Liu DB, Hu JT, Li BL, Ke Y (2019) Efficiency and mechanism of sorption of low concentration uranium in water by powdery aerobic activated sludge. Ecotoxicol Environ Saf 180:483–490
97. Dubinin MM, Radushkevich LV (1947) Equation of the characteristic curve of activated charcoal. Proc Acad Sci Phys Chem Sec USSR 55:331–333
98. Al-Anber ZA, Al-Anber M (2008) Adsorption of ferric ions from aqueous solution by olive cake: thermodynamic and kinetic studies. J Mexican Chem Soc 52:108–115
99. Huynh J, Palacio R, Safizadeh F, Lefèvre G, Descostes M, Eloy L, Guignard N, Rousseau J, Royer S, Tertre E, Batonneau-Gener I (2017) Uranium in water adsorption over NH_2 functionalized ordered silica. ACS Appl Mater Interfaces 9:15672–15684
100. Lagergren S (1898) About the theory of so-called adsorption of soluble substances. Kungliga Svenska Vetenskapsakademiens Handlingar 24:1–39
101. Wong YC, Szeto YS, Cheung WH, McKay G (2004) Pseudo-first-order kinetic studies of the sorption of acid dyes onto chitosan. Appl Polym 92:1633–1645
102. Ho YS, McKay G (1999) Pseudo-second order model for sorption processes. Process Biochem 34:451–465
103. Ho YS, Ofomaja AE (2006) Kinetic studies of copper ion adsorption on palm kernel fiber. J Hazard Mater B137:1796–1802
104. Weber WJ, Morris JC (1963) Kinetics of adsorption on carbon from solution. J Sanit Eng Div 89:31–60